DOI: 10.1002/ejic.200900636

# Metalloamphiphiles with $[Cu_2]$ and $[Cu_4]$ Headgroups: Syntheses, Structures, Langmuir Films, and Effect of Subphase Changes

**Sarmad Sahiel Hindo,[a] Rajendra Shakya,[a] Rama Shanmugam,[a] Mary Jane Heeg,[a] and Cláudio N. Verani*[a]**

**Keywords:** Amphiphiles / Copper / Terephthalate / Pseudomacrocyclic / Langmuir films / Brewster angle microscopy / N,O ligands / Interfaces

The metalloamphiphiles $[(L^{PM18})_2Cu_2Cl_2]\cdot H_2O$ (**1**), $[(L^{PMtax})_2Cu_2Cl_2]\cdot 2MeOH$ (**2**), $[(L^{OF18})_2Cu_2Cl_2]$ (**3**), $[(L^{OF18})_2Cu_4(\mu_4\text{-}O)(\mu_2\text{-}OAc)_4]$ (**4**), $[(L^{OF14})_2Cu_4(\mu_4\text{-}O)(\mu_2\text{-}OAc)_4]$ (**5**) were synthesized and characterized by means of several spectroscopic and spectrometric methods. The acronyms $L^{PMC18}$, $L^{PMtax}$, $L^{OF18}$, and $L^{OF14}$ indicate the deprotonated forms of pseudomacrocyclic (PM) and open-frame (OF) ligands based on 2,6-bis(iminomethyl)-4-methylphenol attached to octadecyl (18), trialkoxyamine (tax) and tetradecyl (14) moieties, whereas $Cl^-$ and $OAc^-$ indicate chlorido and acetato coligands. Crystal structures were obtained for **4** and **5** that crystallize in triclinic crystal systems with $P\bar{1}$ space groups. The average Cu–$O_{phenolate}$ and Cu–$N_{imine}$ bond lengths are approximately 2.0 Å. Species **1**–**5** were analyzed by means of isothermal compression and Brewster angle microscopy (BAM). Moderate collapse pressures of approximately 15 $mN\,m^{-1}$ were observed for **3**, **4**, and **5**, while **1** collapses at approximately 30 $mN\,m^{-1}$. Species **1**, **3**, **4**, and **5** are responsive to several subphase changes such as temperature and addition of terephthalate ions, which leads to considerable Langmuir film enhancement. In presence of terephthalate the collapse pressure for **3**, **4**, and **5** nearly doubles, whereas a minimal effect was observed for **1**. It appears that as temperature decreases, collapse pressure increases. The variation of pH produced inconclusive data. It is suggested that terephthalate ion interacts with the amphiphiles at a molecular level to generate discrete molecules rather than extended systems.



## Introduction

Modern coordination chemistry aims at translating information learned from the study of discrete complexes into useful new materials. Particular attention has been paid to metal-containing soft materials, where metallopolymers,[1] metallomesogens,[2] and metallosurfactants,[3] take advantage of the cooperativity between transition metals and organic scaffolds to build up organized supramolecular architectures with unique geometric, redox, and magnetic properties. Usually, a main aspect of this process is the requirement for such metal-containing soft materials to be organized in highly ordered assemblies, and typically they need to be transfered onto surfaces.

In spite of this growing interest, examples of systems bearing discrete[4] multimetallic cores remain rather limited. Only a few mesogens containing flat multinuclear cores[5,6] and a dendrimeric system supporting an iron–sulfur core[7] have been reported. Recently, we have demonstrated[8] that the use of preassembled carboxylate-based dimers such as copper acetate, formally described as $[Cu_2(OAc)_4(H_2O)_2]$, can overcome this constraint. A synthetic strategy was developed to obtain tetrametallic copper complexes containing $N_2O$-terdentate open-frame ligands based on 2,6-bis-(iminomethyl)-4-methylphenol, $\mu_2$-bridging acetates (or benzoates), and $\mu_4$-oxo groups as coligands. The complexes were characterized spectroscopically and spectrometrically, and their molecular structures were solved; their magnetic properties were determined both experimentally and by means of broken-symmetry DFT calculations; and their mesomorphic and amphiphilic properties were described. Because several transition-metal ions support cluster formation with carboxylate ligands,[9] this methodology constitutes an important starting point.

An alternative way of approaching the development of multimetallic soft materials has been explored by the introduction of bridging ligands or linkers to create extended systems. This approach was used in the development of cyanide-linked magnetic films[10] and bis(terpyridine)-linked hierarchical materials.[11] The magnetic films were obtained by treatment of an amphiphilic pentacyanoferrate complex at the air/water interface with aqueous nickel(II) ions yielding a bidimensional framework, whereas the hierarchical materials were formed by self-assembled polyelectrolyte/amphiphile complexes of poly[iron(II)bis(terpyridine)]/dihexadecyl phosphate.

[a] Department of Chemistry, Wayne State University,
5101 Cass Ave., Detroit, MI 48202, USA
Fax: +1-313-577-8822
E-mail: cnverani@chem.wayne.edu

Supporting information for this article is available on the WWW under http://dx.doi.org/10.1002/ejic.200900636.

   

This article further expands on the coordination chemistry of multinucleating ligands with incorporated hydrophobic chains and their potential for film formation. We present here the synthesis and thorough characterization of novel discrete pseudomacrocyclic and open-frame species containing bimetallic and tetrametallic cores (Scheme 1, counterions and coligands omitted). Studies at the air/water interface with these discrete precursors are followed by evaluation of the effect of the terephthalate (TPA, or 1,4-benzenedicarboxylate) ion on the formation of the resulting Langmuir films. The terephthalate ion has been widely used in the building of metallorganic frameworks[12] and can be dissolved in the aqueous subphase as its sodium salt. Coordination to bimetallic cores and replacement of acetate coligands in tetrametallic cores is expected to happen at the air/water interface, leading to films that might display either discrete substitution or formation of extended frameworks. Under the current conditions, discrete substitution seems to be favored. The results follow.

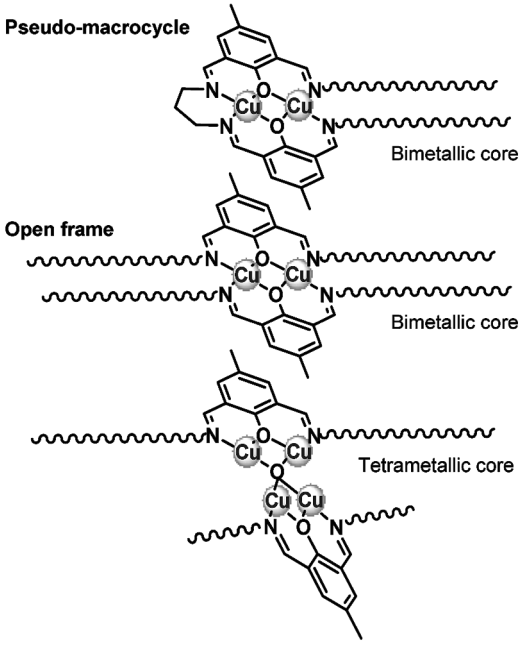


Scheme 1. Pseudomacrocyclic and open-frame $Cu_2$ and $Cu_4$ species. Acetato and chlorido coligands and charges omitted for clarity.

## Results and Discussion

### Design Strategy

The synthetic idea used in this study is to enable the inclusion of multiple copper(II) centers into organic frameworks, with subsequent study of their structural, electronic, and amphiphilic properties. This was accomplished with the design of amphiphiles **1**–**5** (Scheme 2). We begin with **1** and **2**, where two copper(II) centers are coordinated to Robson-type 2,6-bis(iminomethyl)-4-methylphenol[13] pseudomacrocyclic ligands (indicated by the acronym PM in the ligand description) containing distinct chains. Octadecylamine ($C_{18}H_{37}NH_2$) is used in the synthesis of **1**, whereas the trialkoxyamine (tax) 3,4,5-tris(dodecyloxy)aniline is used for **2**. While most electronic properties remain similar, the nature of these distinct chains has strong influence on the amphiphilicity of these systems. Subsequently, **3** is introduced in which two copper(II) centers are coordinated to two ligands that resemble the upper half of a Robson-type macrocycle (indicated as OF, open-frame) with an octadecyl chain bound to each imino nitrogen atom. This species can be compared with **1** in terms of closed-frame vs. open-frame networks. Complexes **4** and **5** resemble previously published carboxylato-based tetracupric structures,[8] where the former has four octadecyl chains ($C_{18}H_{37}$) and the latter has four tetradecyl chains ($C_{14}H_{29}$). Therefore, a comparison is possible between **1**, **3**, and **4** in terms of changing the metal-to-chain ratio. Lastly, the effect of chain-length variation is studied in **4** and **5**.

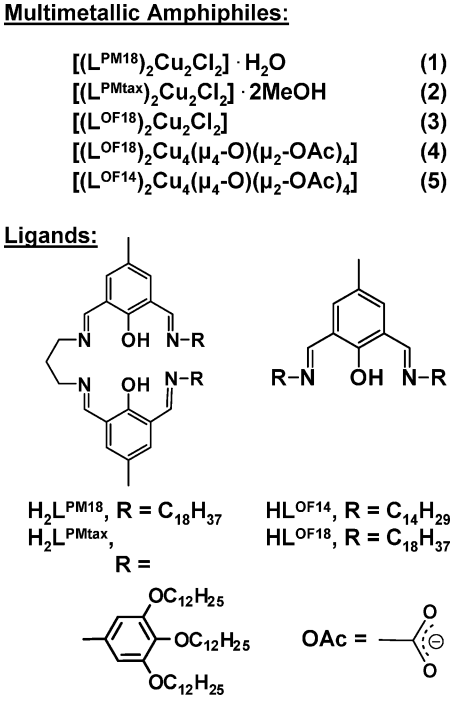


Scheme 2. The copper amphiphiles **1**–**5**.

### Syntheses and Characterizations

The bimetallic **1** and **2** were synthesized from a monometallic [($L^{PMald}$)Cu] aldehyde precursor, as usual for such systems.[13,14] The compounds were thoroughly characterized by infrared spectroscopy, ESIMS spectrometry, and elemental analysis. The IR feature for **1** showed the disappearance of C=O stretches at 1670 $cm^{-1}$, and appearance of a new peak for the C=N stretch at 1634 $cm^{-1}$, along with the peaks at 2850–2918 $cm^{-1}$ attributed to C–H stretches of the alkyl chains. These changes are indicative of the metal template-supported reaction between an in situ formed [($L^{PMald}$)$Cu_2$] precursor and octadecylamine, thereby generating the desired [($L^{PM18}$)$_2Cu_2Cl_2$]·$H_2O$ (**1**). The ESI mass analysis in the positive mode gave the 100% peak at 1027 for [**1** – Cl]$^+$ species. Analogous IR and ESIMS behavior

  

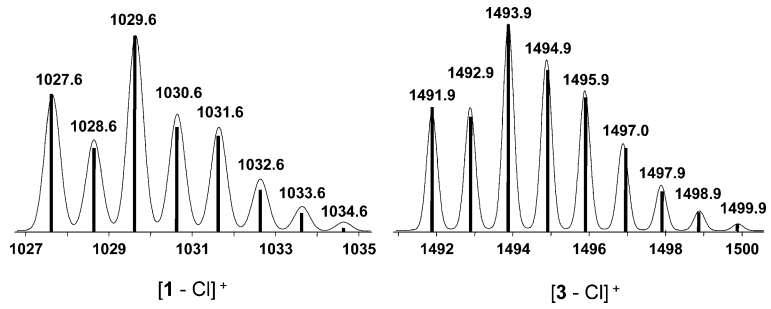


Figure 1. ESI(pos) peak clusters for **1** and **3**: $[M - Cl^-]^+$.

was observed for **2**. The ESIMS peaks for **1** and **2** were simulated giving well defined isotopic distribution patterns in good agreement with the calculated values. A selected example is shown in Figure 1.

Compounds **3** to **5** were synthesized by using the open-frame bis(imino*alkyl*)-4-methylphenol $HL^{OFn}$ ligands ($n$ = 18 and 14 for octadecyl and tetradecyl, respectively). These species were prepared by Schiff condensation of the precursor 2,6-diformyl-4-methylphenol with octadecylamine and tetradecylamine. The precursor was obtained in an analogous way as the previously published 4-*tert*-butyl-2,6-diformylphenol.[8] The ligands $HL^{OF18}$ and $HL^{OF14}$ were thoroughly characterized by $^1H$ NMR and IR spectroscopy, as well as by ESI-MS analysis. The most diagnostic $^1H$-NMR peak for the ligands is a multiplet at approximately 1.25 ppm associated with the C–H groups of the side alkyl chains. Similarly, the IR spectrum verifies the C=N nature of the ligands displaying peaks at approximately 1640 $cm^{-1}$. Observed ESIMS peaks at $m/z$ = 667.6 and 555.4 account for the $[HL^{OFn} + H]^+$ species. The bimetallic **3** was synthesized by treatment of $HL^{OF18}$ with a methanol solution of copper(II) chloride in a 1:1 (L:Cu) molar ratio. The evidence of the complex formation is given by the ESIMS data with a peak at $m/z$ = 1492 related to $[\mathbf{3}–Cl]^+$. This peak showed the expected isotopic distribution associated with copper ions, as in Figure 1. The tetrametallic complexes **4** and **5** were synthesized by respective treatment of an ethanol solution of $HL^{OF18}$ or $HL^{OF14}$ with copper(II) acetate in a 1:2 (L:Cu) molar ratio. These compounds were isolated as dark green colored crystals and analyzed by ESIMS. Evidence was gathered for the $[Cu_2L^{OFn}(OAc)_2]^+$ fragments, and isotopic distributions were comparable to those previously observed for similar μ-oxo $Cu_4$ analogues.[8] The elemental analyses of **1** to **5** are in very good agreement with the suggested structures.

## Description of the Structures

Molecular structures were not obtained for **1**–**3**, because of the lack of suitable single crystals. Nonetheless, the analysis allows for direct comparison to other well established structures.[14] The molecular structures of **4** and **5**

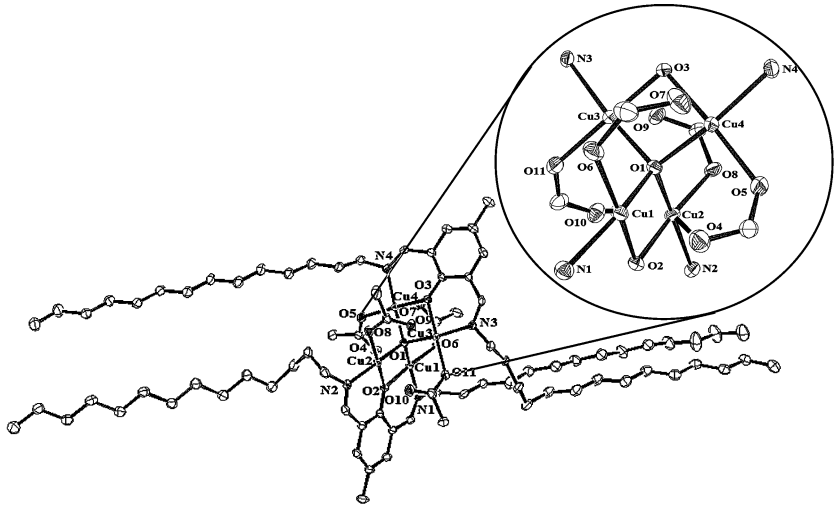


Figure 2. ORTEP diagrams for **5** with the $[(\mu_4\text{-}O)(\mu_2\text{-}OAc)_4Cu_4]$ core. Selected bond lengths [Å] and angles (°): Cu(1)–O(1) 1.9259(13), Cu(1)–O(6) 1.9472(14), Cu(1)–O(2) 1.9889(13), Cu(1)–N(1) 1.9950(17), Cu(1)–O(4) 2.2246(15), Cu(1)–Cu(2) 3.0004(4), Cu(2)–O(1) 1.9153(13), Cu(2)–O(8) 1.9354(14), Cu(2)–N(2) 1.9791(16), Cu(2)–O(2) 1.9877(13), Cu(2)–O(10) 2.3855(15), Cu(3)–O(1) 1.9164(13), Cu(3)–O(11) 1.9457(15), Cu(3)–N(3) 1.9710(16), Cu(3)–O(3) 1.9714(14), Cu(3)–O(9) 2.3847(14), Cu(3)–Cu(4) 2.9975(4), Cu(4)–O(1) 1.9196(13), Cu(4)–O(5) 1.9426(14), Cu(4)–N(4) 1.9870(17), Cu(4)–O(3) 1.9898(13), Cu(4)–O(7) 2.2170(15), Cu(2)–O(1)–Cu(3) 110.82(7), Cu(2)–O(1)–Cu(4) 117.60(7), Cu(3)–O(1)–Cu(4) 102.78(6), Cu(2)–O(1)–Cu(1) 102.72(6), Cu(3)–O(1)–Cu(1) 112.60(6), Cu(4)–O(1)–Cu(1) 110.66(7).

  

were determined by X-ray diffraction, and the ORTEP plot of **5**, with selected average bond lengths and angles, is shown in Figure 2. Complex **5** is composed of a discrete neutral molecule consisting of two deprotonated ligands $(L^{OF14})^-$, each of them delivering a set of $N_2O$ donor atoms to a cluster of four copper(II) centers $\mu_4$-bridged by a distorted tetrahedral oxygen atom. Four acetato coligands complete the coordination sphere. The oxygen atoms from each phenolate ring bridge two copper(II) ions that lie at approximately 2.0 Å from each other. The Cu–O–Cu angles reach 102–118°, and the four Cu–$N_{imine}$ bonds are approximately 1.97 Å in length. The ORTEP plot of the complex **4** is similar to that of **5** and is shown in the Figure S1 (Supporting Information) with selected bond lengths and angles. Both structures resemble closely those from previously published species.[8]

### Behavior at the Air/Water Interface

The amphiphilic properties of **1**–**5** were evaluated by means of compression isotherms by plotting surface pressure (Π, mN m$^{-1}$) vs. average area per molecule [*A* (Å)$^2$] and Brewster angle microscopy (BAM). Compression isotherms were performed at compression rates of 5 mm min$^{-1}$ for **2**, **3**, **4**, and **5**, as well as at 5 and 10 mm min$^{-1}$ for **1**. As shown in Figure 3, at a faster compression rate, individual molecules of both **1** and **2** start interacting when average molecular areas reach approximately 110 Å$^2$. This value coincides roughly with the expected area of the pseudomacrocyclic bimetallic core, estimated by using a molecular mechanics MM2 model. Slower rates allow for decreased average areas, perceived as an improvement in the molecular packing for **1**. Both amphiphiles appear to collapse at approximately 50–70 mN m$^{-1}$, although closer examination of the 5 mm min$^{-1}$ compression isotherm for **1**, along with BAM data, indicate profuse formation of granular domains and Newton rings[15] after 25–30 mN m$^{-1}$. This is suggestive of multilayer formation, likely to be related with camshaft-like motions of the alkyl and alkoxy chains. These domains are apparent even at lower surface pressures for **2**. Subtle inflections in the compression isotherm of this compound are observed around 5–10 mN m$^{-1}$, thus limiting considerably the quality and reproducibility of the resulting films. The instability of films for **2** is probably associated to the bulkiness and disorder of multibranched trialkoxy groups. As a matter of fact, another copper amphiphile developed by our group using the same alkoxy motif has shown similar limitations.[16] No further studies where carried out for **2**.

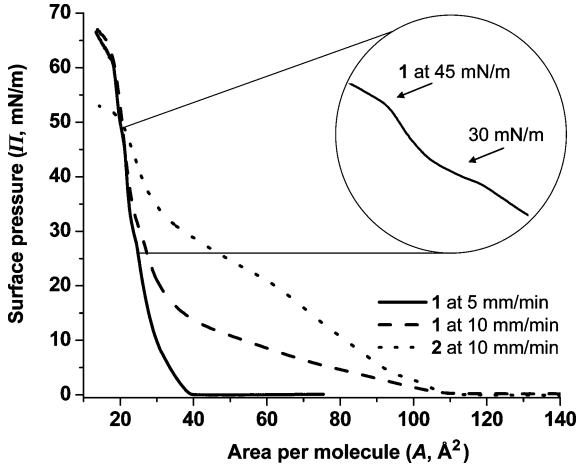


Figure 3. Isotherms of **1** at 5 and 10 mm min$^{-1}$ and **2** at 10 mm min$^{-1}$ compression rates.

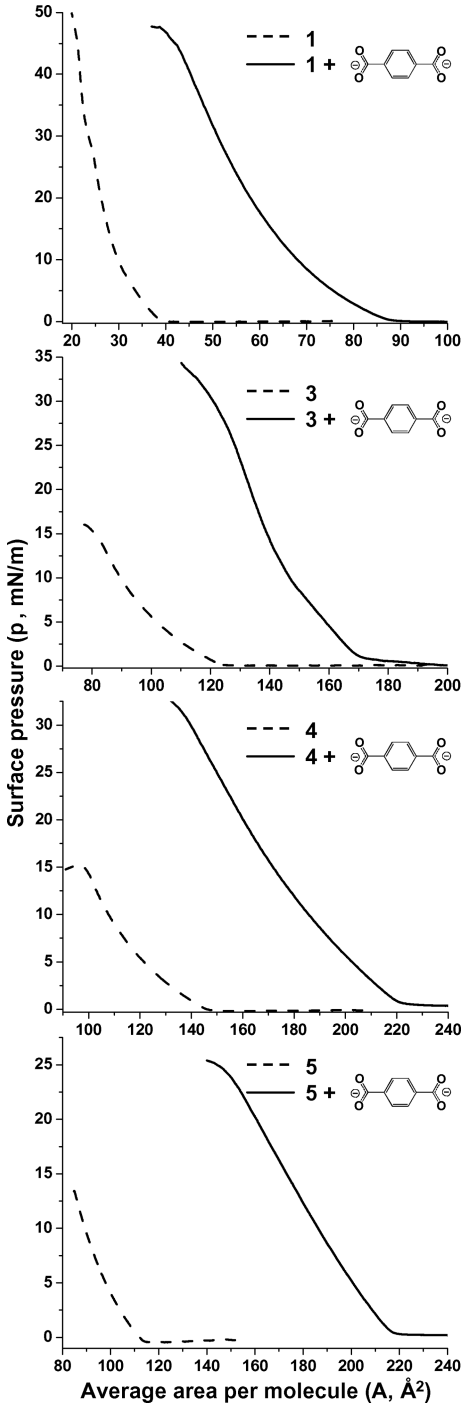


Figure 4. Isotherms of **1**, **3**, **4**, and **5** at room temperature, pH 7 (dotted line), and room temperature, pH 7 with $Na_2TPA$ (solid line).

  

The compression isotherms for **4**–**5** resemble closely those previously reported for μ-oxo $Cu_4$ species with equivalent ligands,[8b] showing average collapse areas of 110–130 $Å^2$ and slightly improved collapse pressures from approximately 10 to 15 $mN\,m^{-1}$. The main difference between these and the previously published $N_2O$ terdentate ligands is the replacement of a *tert*-butyl by a methyl group at the *para* position of the phenolate ring. Therefore it can be inferred that the improved collapse pressures reflect the presence of a smaller, less hydrophobic substituent. The increased area for **4**–**5** when compared to **1** reflects a slightly augmented core revealing the tetrahedral nature of the tetrametallic core. As expected, the average molecular area at collapse for the bimetallic **3** is larger than that observed for **1** but slightly smaller than that of **4**. It can be concluded that the presence of opposing chains limits the packing for the open-frame structures of **3**–**5**. These data are summarized along with the effect of linkers and temperature changes in Figure 4.

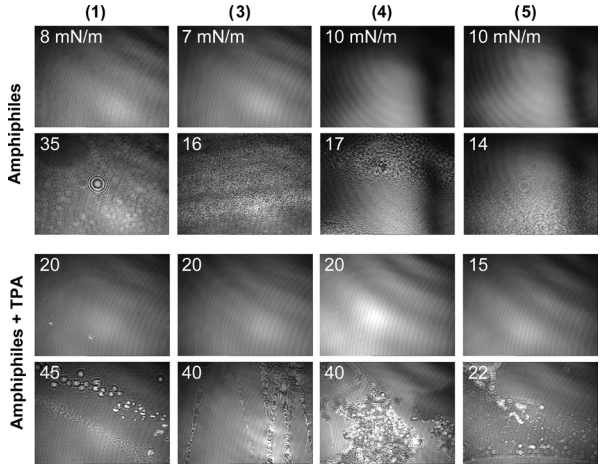


Figure 5. Selected BAM of **1**, **2**, **3**, and **5** at room temperature and pH 7 for the individual amphiphiles (top) and after addition of disodium terephthalate (bottom). All values indicated at the upper leftmost corner of the individual micrographs are given in $mN\,m^{-1}$.

### Effect of Subphase Changes

Aiming at improved film formation, the effect of disodium terephthalate ($Na_2TPA$) was evaluated at different temperatures and pHs. The ion TPA is the doubly deprotonated dianion of 1,4-benzenedicarboxylic acid and has been used in the building of metallorganic frameworks due to its capability of linking multiple metal centers.[12] The $Cu_2$ and the μ-oxo $Cu_4$ cores can coordinate to the terephthalate ion with potential formation of more hydrophilic discrete amphiphiles or extended coordination polymers at the air/water interface. The reactivity toward terephthalate species becomes particularly relevant for the μ-oxo $Cu_4$ cores, where acetate-by-terephthalate ligand exchange can take place. Therefore, a 0.1 M disodium terephthalate aqueous subphase was used in attempts to enhance the stability and increase the surface pressures at collapse of the resulting films.

As depicted in Figure 4, it can be observed that this ion nearly doubles the formal collapse pressure of **3**, **4**, and **5**, reaching approximately 30 $mN\,m^{-1}$. In principle, a less obvious result takes place for **1**, where the linker seems to decrease the collapse pressure of the pseudomacrocyclic species. However, BAM comparison for **1** in the presence and absence of the terephthalate ion is quite instructive: Observed Newton rings indicative of multilayer formation after 25–30 $mN\,m^{-1}$ give place to an enhanced and smooth film upon incorporation of the terephthalate ion (Figure 5). In addition, it is observed that the average area per molecule increases, thus suggesting that the ion interacts with the amphiphiles. The average area of a flat terephthalate ion can be estimated by MM2 modeling as being around 20–25 $Å^2$. The average areas increase approximately by 40 $Å^2$ for **1**, 60 $Å^2$ for **3** and **4**, and 90 $Å^2$ for **5**, thus suggesting the association of more than one TPA ion per molecule of amphiphile. This number nears two TPA for **1**, two to three for **3** and **4**, and up to four in **5**.

Interfacial changes were also studied using Brewster angle microscopy. The BAM micrographs for **1**, **3**, **4**, and **5** at 23 °C and pH 7 are displayed in Figure 5 and **S2** (expanded view). The pure amphiphiles at the air/water interface are shown in Figure 5 (top), whereas the effect of TPA addition is depicted at the bottom of this graphic. It can be seen that at low surface pressures of 7–10 $mN\,m^{-1}$ the Langmuir films of **3**, **4**, and **5** show a smooth homogeneous surface. However when the surface pressure is increased to approximately 14–17 $mN\,m^{-1}$, an increasing roughness of the film leads to the formation of several Newton rings and spherical domains. A gentle tipping of the isotherms can be observed for **3**, **4**, and **5** indicating collapse with further multilayer formation. Complex **1** shows these multiple domains after 35 $mN\,m^{-1}$. These BAM results correlate well with the observed behavior for the isothermal compressions.

As observed in the compression isotherms in Figure 4, addition of sodium terephthalate revealed that there is an evident enhancement in amphiphilicity for systems **1**, **3**–**5**. It can be seen that the presence of TPA yielded more homogeneous Langmuir films up to approximately 40 $mN\,m^{-1}$. Interestingly, the formal collapse observed previously is not visible. A gradual decrease in the slope of the curve appears after 45 $mN\,m^{-1}$ for **1**, 40 $mN\,m^{-1}$ for **3** and **4**, and 22 $mN\,m^{-1}$ for **5**. It seems reasonable to conclude that the addition of the terephthalate ion has influenced the monolayer stability and surface area. Therefore, it can be suggested that the ion TPA,at this concentration, interacts with the individual amphiphiles.[17]

Having shown the film dependence on the presence of terephthalate at 23 °C, we evaluated the effect of temperature and pH change on these systems. The compression isotherms and BAM for **1**, **3**, **4**, and **5** were measured at 13 and 33 °C and neutral pH, in the presence of disodium terephthalate. Selected isotherms and BAM for **4** are shown in Figure 6 and reveal a particular trend in amphiphilic be-

  

havior; as temperature decreases, there is an increase in the collapse pressure followed by formation of multilayers. Figure S3 (Supporting Information) displays similar data for **5**. Therefore, a change in 20 °C corresponds to a comparable change of 20 mN m$^{-1}$ for **4** in the collapse inflection point. The effect temperature has on the amphiphilic behavior is commonly correlated to Brownian motion of molecules in Langmuir films.[18] Available literature suggest an explanation on how an increase in temperature is related to an increase in the collapse pressure in traditional amphiphiles.[19–21] The increase in collapse pressure is attained due to the elevated Brownian motion occurring at higher temperatures which stabilizes the expanded phase. Considerably less is known pertaining to the influence of temperature on the amphiphilic behavior of non-traditional metalloamphiphiles and a reverse amphiphilic effect – a temperature increase results in a collapse pressure decrease – can be observed. Such effect has been reported when metals are incorporated into organic systems, where Kang et al.[22] report a noticeable increase in collapse pressure at the air/water interface for stearic acid on a γ-$Fe_2O_3$ nanoparticle subphase as the temperature decreases from 20–5 °C. A similar effect has been observed here, suggesting that for these systems, as the temperature of the subphase decreases there is an observed increase in the collapse pressure.[23] Brewster angle microscopy reinforces this notion by showing comparable behavior for **2**, **3**, **4** and **5**. At low temperatures, homogeneous films were observed at higher collapse pressures, whereas at 33 °C proliferation of Newton rings become evident at approximately 20 mN m$^{-1}$. Changes in the pH of the subphase were inconclusive. Acidic conditions were avoided to prevent ligand reprotonation and fragmentation of the cluster core, while at pH 9 inconclusive data was gathered. It is possible that basic pH values support copper-catalyzed imine hydrolysis.[24]

Analysis of the isothermal compression and BAM data allow for some generalizations, as follows: For the bimetallic **1** and **3**, if an extended framework were to be observed, a linear topology should be adopted and the average area increase should correspond to the addition of a single TPA/amphiphile. Therefore, we suggest that whereas coordination of the terephthalate ion to the metal core seems to take place, it is likely to yield discrete molecules rather than extended linear frameworks at this TPA:amphiphile ratio. It is probable that the flat [$Cu_2$] headgroups support coordination of terephthalates dissolved in the water subphase as suggested in the simplified model shown in part a of Scheme 3 where multiple TPA ions are present, rather than as in part b where the expected area increase should reflect the coordination of a single TPA ion per amphiphile.

For the tetrametallic **4** and **5**, one to four terephthalate ions could be associated, depending on the degree of acetate-by-terephthalate substitution at the core of these species. Close examination of the [$Cu_4$] core in the inset of Figure 2 suggests that extended framework formation will be primarily favored when (i) at least one acetato coligand is replaced by a TPA ion per core, and assuming they (ii) align themselves within the water surface plane as shown in Scheme 4 (b, iii) coming to close contact to allow core linking. Because the TPA ions are dissolved in water, their orientation – and possibly concentration – are not optimized and the two last requirements are not favored. Vicinal acetato coligands at the [$Cu_4$] core should be more easily replaced, as suggested in the simplified model shown in Scheme 4 (a).

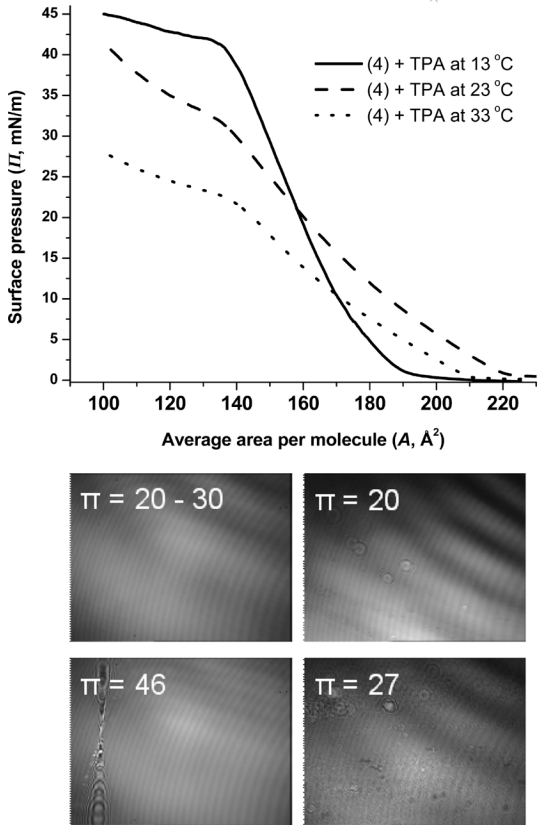


Figure 6. Top: isotherms of **4** at 13, 23, and 33 °C, pH 7, with disodium terephthalic salt. Bottom: selected BAM micrographs for **4** at a) 13 and b) 33 °C.

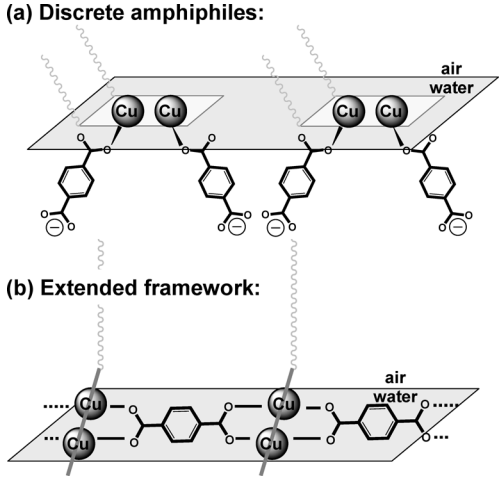


Scheme 3. Discrete and extended configurations of [$Cu_2$] headgroups interacting with terephthalate ions at the air/water interface.

  

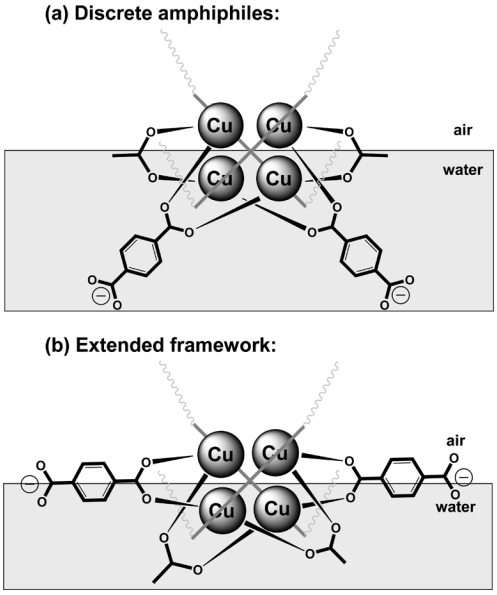


Scheme 4. Discrete and extended configurations of $[Cu_4]$ headgroups interacting with terephthalate ions at the air/water interface.

We suggest that the increased formal collapse observed upon addition of terephthalates to the water subphase is supported by an increase in the hydrophilicity of the $[Cu_2]$ and $[Cu_4]$ cores, rather than being due to the formation of extended frameworks. The latter case may be favored at different TPA concentrations. The investigation of these topologies requires further study, either by X-ray reflectivity[25] of the Langmuir film or by probing differences in molecular order of the equivalent Langmuir–Blodgett films by sum frequency generation[26] However, these techniques are not available at this time.

## Conclusions

We have demonstrated previously that copper-containing clusters can be incorporated in amphiphilic frameworks. However, modest collapse pressures were a limiting factor. In this article we have explored (i) different core sizes, (ii) structural architectures, and (iii) subphase changes to address this problem. We synthesized the pseudomacrocyclic and open-frame bimetallic species **1**, **2**, and **3**, along with the $\mu_4$-oxo supported open-frame tetrametallic cuproamphiphiles **4** and **5**. An evaluation of their ability to form Langmuir films indicated persisting moderate surface pressures, and in order to overcome this limitation we tested the effect of terephthalate ions along with temperature and pH changes for the enhancement of film formation. The terephthalate ions seem capable of coordination to the copper core either by replacement of chlorido coligands in **1**, **2**, and **3**, or acetato coligands in **4** and **5**. This interaction can lead to either discrete species with enhanced hydrophilicity or extended frameworks. The connectivity of the bimetallic moiety by a linker has been demonstrated recently by Andruh and collaborators,[27] although it is still to be realized in tetrametallic frameworks. On basis of the observed experimental data we conclude that the larger average areas per molecule observed for **1**, **3**, **4**, and **5** in presence of terephthalates support substitution of the core coligands in individual molecules. At this point we favor the formation of discrete species rather than extended frameworks. Ongoing research focuses on changing the concentration of TPA at the water subphase. Targeting of extended frameworks will be attempted by the synthesis of copper-terephthalate precursors for reaction and isolation of $\mu_4$-oxo supported open-frame tetrametallic amphiphiles.

## Experimental Section

**Materials and Methods:** Reagents and solvents were used as received from commercial sources. Dichloromethane was purified in an Innovative Technologies solvent purification system using alumina columns. Methanol and ethanol were distilled from $CaH_2$. Infrared spectra were measured on a Bruker Tensor 27 FTIR spectrophotometer from 4000 to 400 $cm^{-1}$ as KBr pellets. $^1H$ NMR spectra were measured with a Varian 400 mHz instrument. ESI spectra were measured with a Micromass QuattroLC triple quadrupole mass spectrometer with electrospray/APCI source and Walters Alliance 2695 LC, autosampler and photodiode array UV detector. Experimental assignments were simulated based on peak position and isotopic distributions. Melting points were determined with a Fisher-Johns apparatus and elemental analyses were performed by Midwest Microlab, Indianapolis, IN.

**X-ray Structural Determinations for 4 and 5:** Diffraction data were measured with a Bruker APEX-II Kappa geometry diffractometer with Mo radiation and a graphite monochromator at 100 K. Frames were collected with the detector at 40 mm, 0.3° between each frame and 30 or 5 s/frames, respectively, for **4** $[C_{98}H_{174}Cu_4N_4O_{11}]$ and **5** $[C_{82}H_{142}Cu_4N_4O_{11}]$. All frame data was indexed and integrated with SMART, SAINT and SADABS software[28] provided by the manufacturer. The models were refined using Sheldrick's SHELX-97 software.[29] The neutral molecules crystallized without solvent or counterions. Three atoms in the pendant chains in **5** (C15, C17 and C19) were assigned partial occupancy sites and refined isotropically. Table 1 lists the experimental

Table 1. Crystal data for **4** and **5**.[a]

| Complex | **4** | **5** |
|---|---|---|
| Empirical formula | $C_{98}H_{174}Cu_4N_4O_{11}$ | $C_{82}H_{142}Cu_4N_4O_{11}$ |
| Formula weight | 1838.57 | 1614.16 |
| Temperature | 100(2) | 100(2) K |
| Wavelength | 0.71073 Å | 0.71073 Å |
| Crystal system, space group | triclinic, $P\bar{1}$ | triclinic, $P\bar{1}$ |
| Unit cell dimensions | $a$ = 12.8632(8) Å | $a$ = 12.8538(6) Å |
| | $b$ = 16.8119(11) Å | $b$ = 16.8960(8) Å |
| | $c$ = 24.1373(17) Å | $c$ = 21.6180(10) Å |
| | $\alpha$ = 104.132(2)° | $\alpha$ = 69.377(2)° |
| | $\beta$ = 93.705(2)° | $\beta$ = 76.815(2)° |
| | $\gamma$ = 97.786(2)° | $\gamma$ = 81.551(2)° |
| Volume | 4989.2(6) $Å^3$ | 4266.8(3) $Å^3$ |
| $Z$, calculated density | 2, 1.224 $Mg/m^3$ | 2, 1.256 $Mg/m^3$ |
| Absorption coefficient | 0.898 $mm^{-1}$ | 1.040 $mm^{-1}$ |
| Final $R$ indices $[I>2\sigma(I)]$ | $R_1$ = 0.0672, | $R_1$ = 0.0396, |
| | $wR_2$ = 0.1271 | $wR_2$ = 0.0943 |
| $R$ indices (all data) | $R_1$ = 0.1623, | $R_1$ = 0.0396, |
| | $wR_2$ = 0.1533 | $wR_2$ = 0.0943 |

[a] $R(F) = \sum||F_o| - |F_c||/\sum|F_o|$; $R_w(F) = [\sum w(F_o^2 - F_c^2)^2/\sum w(F_o^2)^2]^{1/2}$ for $I>2\sigma(I)$.

  

parameters.CCDC-747590 (for **4**) and -747591 (for **5**) contain the supplementary crystallographic data for this paper. These data can be obtained free of charge from the Cambridge Crystallographic Data Centre via www.ccdc.cam.ac.uk/data_request/cif.

**Compression Isotherms:** The *Π-A* isotherms were measured in an automated KSV 2000 minitrough at variable temperature. Ultrapure water (Barnstead NANO pure) was used for all experiments with a resistivity of 17.5–18 MΩ cm$^{-1}$. Adventitious impurities at the surface of freshly poured aqueous subphases were removed by vacuum after barrier compression. Spreading of a known quantity (ca. 30 μL) of 1.0 mg mL$^{-1}$ chloroform solutions on the aqueous subphase was followed by 20 min equilibrium time before monolayer compression. The isotherms were obtained at a compression rate of 5 or 10 mm min$^{-1}$, as described in the text. The pressure was measured using the Wilhelmy plate method (platinum plate, 40 mm perimeter). At least three independent measurements were carried out per sample with excellent reproducibility.

**Brewster Angle Microscopy:** A KSV-Optrel BAM 300 with a HeNe laser (10 mW, 632.8 nm) and a CCD detector was used in all micrographs. The compression rate was 5 mm min$^{-1}$, the field of view was 800 × 600 microns, and the lateral resolution was 2 μm.

**Syntheses**

**Preparation of the Precursors:** 2,6-Diformyl-4-methylphenol ($C_9H_8O_3$, 164.16 g/mol),[30] 3,4,5-tris(dodecyloxy)aniline, ($C_{42}H_{78}NO_3$, 645.07 g/mol)[31] and [($L^{PMald}$)Cu] ($C_{21}H_{20}CuN_2O_4$, 427.94 g/mol)[32] were prepared by adapting reported literature.

**Preparation of the Ligands $HL^{OF18}$ and $HL^{OF14}$:** 1-Octadecylamine (1.08 g, 0.4 mmol) was added to a hot solution of 2,6-diformyl-4-methylphenol (0.33 g, 0.2 mmol) in 30 mL ethanol to obtain $HL^{OF18}$ and 1-tetradecylamine (1.10 g, 0.4 mmol) for $HL^{OF14}$. The mixture was refluxed for 1 h when a dark yellow product was formed. The yellow precipitate was isolated by suction filtration after 12 h at 0 °C, washed with cold ethanol, and dried under vacuum.

**$HL^{OF18}$:** Yield 1.10 g, 83% for [$C_{45}H_{82}N_2O$] (667.15 g/mol). $^1$H NMR spectroscopic data (400 MHz, $CDCl_3$, 300 K): $\delta$ = 0.88 [m, 6 H, (2-$CH_3$)], 1.25 [m, 56 H (chain-$CH_2$)], 1.70 [m, 4 H, 2 (C=N-$CH_2$-$CH_2$-)], 2.30 [1s, 3 H, (methyl-$CH_3$)], 3.59 [m, 4 H, 2 (C=N-$CH_2$-)], 7.26 [1s, 2 H, (aryl)], 8.29 [1s, 2 H, (CHN)] ppm. IR data (KBr): $\tilde{\nu}$ = 1640 ($\nu_{C=N}$), 2850–2950 ($\nu_{C-H}$ from alkyl chain and methyl groups) cm$^{-1}$. MS data (ESI$^+$, MeOH): *m*/*z* = 667.6 [$HL^{OF18}$ + H]$^+$.

**$HL^{OF14}$:** Yield 0.90 g, 79% for [$C_{37}H_{66}N_2O$] (554.93). $^1$H NMR spectroscopic data (400 MHz, $CDCl_3$, 300 K): $\delta$ = 0.90 [m, 6 H, (2-$CH_3$)]; 1.28 [m, 56 H (chain-$CH_2$)], 1.74 [m, 4 H, 2 (C=N-$CH_2$-$CH_2$-)], 2.41 [1s, 3 H, (methyl-$CH_3$)]; 3.61 [m, 4 H, 2 (C=N-$CH_2$-)], 7.21 [1s, 2 H, (aryl)], 8.33 [1s, 2 H, (CHN)] ppm. IR data (KBr): $\tilde{\nu}$ = 1641 ($\nu_{C=N}$), 2850–2920 ($\nu_{C-H}$ from alkyl chain and methyl groups) cm$^{-1}$. MS data (ESI$^+$, MeOH): *m*/*z* = 555.4 [$HL^{OF14}$ + H]$^+$.

**Preparation of the Metalloamphiphiles [($L^{PM18}$)$_2$$Cu_2Cl_2$]·$H_2O$ (1) and [($L^{PMtax}$)$_2$$Cu_2Cl_2$]·2MeOH (2):** $CuCl_2$·2$H_2O$ (0.10 g, 0.5 mmol) dissolved in a minimum amount of methanol was added dropwise to a homogeneous suspension of [($L^{PMald}$)Cu] (0.22 g, 0.5 mmol) in methanol (20 mL). A clear green solution formed immediately and was stirred for 20 min, when 2 equiv. of octadecylamine (0.27 g, 1 mmol) for **1** or tris(dodecyloxy)aniline (0.645 g, 1 mmol) for **2** were added. A clear solution was formed and gently refluxed for 1 h. After cooling to room temperature amorphous to globular precipitates were isolated, washed with pentane and dried under vacuum.

**1:** Yield 0.45 g, 79%. $C_{57}H_{96}Cl_2Cu_2N_4O_3$ (1083.41 g/mol): calcd. C 63.19, H 8.93, N 5.17; found C 63.11, H 8.78, N 5.09; m.p. 158 °C. IR data (KBr): $\tilde{\nu}$ = 3394 (broad, O–H from $H_2O$) 2917(s), 2850 (s) (C– H from alkyl chain), 1634 (s) (C=N), 1455 (s) (C=C, ar), 1278 (s) (C–O) cm$^{-1}$. MS data (ESI$^+$, MeOH): *m*/*z* = 1027.6 for [**1** – Cl]$^+$.

**2:** Yield 0.67 g, 69% . $C_{107}H_{182}Cl_2Cu_2N_4O_{10}$ (1882.64 g/mol). calcd. C 68.26; H, 9.74; N, 2.98%; found C, 68.17; H, 9.69; N, 3.01%; m.p. 132 °C. IR data (KBr): $\tilde{\nu}$ = 2923 (s), 2853 (s) (C–H from alkyl chain), 1631 (s) (C=N), 1467 (s) (C=Npy, C=C, ar), 1231 (s) (C–O) cm$^{-1}$. MS data (ESI$^+$, MeOH): *m*/*z* = 1780.0 for [**2** – Cl]$^+$.

**Preparation of the Metalloamphiphiles [($L^{OF18}$)$_2$$Cu_2Cl_2$] (3), [($L^{OF18}$)$_2$$Cu_4$($\mu_4$-O)($\mu_2$-OAc)$_4$] (4), and [($L^{OF14}$)$_2$$Cu_4$($\mu_4$-O)($\mu_2$-OAc)$_4$] (5):** A solution of **$HL^{OF18}$** (0.33 g, 0.5 mmol) in 50 mL of methanol was treated with $CuCl_2$·2$H_2O$ (0.10 g, 0.5 mmol) to obtain **3** or $Cu(OAc)_2$·$H_2O$ (0.20 g; 1.0 mmol) for **4**. A solution of **$HL^{OF14}$** (0.32 g, 0.5 mmol) in 40 mL of ethanol was treated with $Cu(OAc)_2$·$H_2O$ (0.20 g, 1.0 mmol). The resulting solutions were refluxed for 1 h yielding a green solution that was cooled down to room temperature. A light green precipitate for **3** was formed and isolated by filtration. Dark green rod-shaped crystals suitable for X-ray analysis were obtained for **4** and **5** upon slow evaporation of the solvent.

**3:** Yield 0.49 g, 65%. $C_{90}H_{162}Cl_2Cu_2N_4O_2$ (1530.30): calcd. C 70.64, H 10.67, N 3.66; found C 70.36, H 10.61, N 3.58; m.p. 148 °C. IR data (KBr): $\tilde{\nu}$ = 1637 ($\nu_{C=N}$), 2852–2918 ($\nu_{C-H}$ from alkyl chain and methyl groups) cm$^{-1}$. MS data (ESI$^+$, MeOH): *m*/*z* = 1491.9 for [**3** – Cl]$^+$.

**4:** Yield 0.68 g, 75%. $C_{98}H_{174}Cu_4N_4O_{11}$ (1838.57): calcd. C 64.02, H 9.54, N 3.05; found C 64.13, H 9.49, N 3.11; m.p. 190 °C. IR data (KBr): $\tilde{\nu}$ = 1629 ($\nu_{C=N}$), 2852–2921 ($\nu_{C-H}$ from alkyl chain and methyl groups) cm$^{-1}$. MS data (ESI$^+$, MeOH): *m*/*z* = 909.52 for [$Cu_2L^{OF18}(OAc)_2$]$^+$.

**5:** Yield 0.72 g, 77%. $C_{82}H_{142}Cu_4N_4O_{11}$ (1614.16): calcd. C 61.01, H 8.87, N 3.47; found C 61.11, H 9.00, N 3.58; m.p. 203 °C. IR data (KBr): $\tilde{\nu}$ = 1640 ($\nu_{C=N}$), 2817–2954 ($\nu_{C-H}$ from alkyl chain and methyl groups) cm$^{-1}$. MS data (ESI$^+$, MeOH): *m*/*z* = 853.5 for [$Cu_2L^{OF14}(OAc)_2$]$^+$.

**Supporting Information** (see also the footnote on the first page of this article): ORTEP diagram for **4** with selected bond lengths [Å] and angles (°), and expanded view of Figure 6, and additional data for temperature-dependent isothermal compression and BAM of **5** are included.

## Acknowledgments

C. N. V. acknowledges the National Science Foundation (NSF) (Grant CHE-0718470) and the Nano@Wayne initiative (Fund 11E420) for financial support.

[1] a) B. J. Holliday, T. M. Swager, *Chem. Commun.* **2005**, 23; b) S. J. Rowan, J. B. Beck, *J. Am. Chem. Soc.* **2003**, *125*, 13922; c) I. Manners, *Science* **2001**, *294*, 1664; d) C. L. Fraser, A. P. Smith, *J. Polym. Sci.* **2000**, *38A*, 4704.

[2] a) E. Terazzi, S. Suarez, S. Torelli, H. Nozary, D. Imbert, O. Mamula, J.-P. Rivera, E. Guillet, J.-M. Bénech, G. Bernardinelli, R. Scopelliti, B. Donnio, D. Guillon, J.-C. Bünzli, C. Piguet, *Adv. Funct. Mater.* **2006**, *16*, 157; b) J. L. Serrano, T. Sierra, *Coord. Chem. Rev.* **2003**, *242*, 73; c) B. Donnio, *Curr. Opin. Colloid Interface Sci.* **2002**, *07*, 371.

  

[3] a) J. Bowers, K. E. Amos, D. W. Bruce, R. K. Heenan, *Langmuir* **2005**, *21*, 5696; b) P. C. Griffiths, I. A. Fallis, D. J. Willock, A. Paul, C. L. Barrie, P. M. Griffiths, G. M. Williams, S. M. King, R. K. Heenan, R. Görgl, *Chem. Eur. J.* **2004**, *10*, 2022; c) J. M. Rueff, N. Masciocchi, P. Rabu, A. Sironi, A. Skoulios, *Eur. J. Inorg. Chem.* **2001**, 2843.
[4] M. Clemente-Leon, E. Coronado, C. J. Gomez-Garcia, C. Mingotaud, S. Ravaine, G. Romualdo-Torres, P. Delhaes, *Chem. Eur. J.* **2005**, *11*, 3979.
[5] a) R. W. Date, E. F. Iglesias, K. E. Rowe, J. M. Elliott, D. W. Bruce, *Dalton Trans.* **2003**, 1914; b) K. Binnemans, K. Lodewyckx, B. Donnio, D. Guillon, *Chem. Eur. J.* **2002**, *8*, 1101; c) T. Hegmann, B. Neumann, J. Kain, S. Diele, C. J. Tschierske, *Mater. Chem.* **2000**, *10*, 2244.
[6] a) J. Szydlowska, A. Krowczynski, E. Gorecka, D. Pociecha, *Inorg. Chem.* **2000**, *39*, 4879; b) R. Paschke, S. Liebsch, C. Tschierske, M. A. Oakley, E. Sinn, *Inorg. Chem.* **2003**, *42*, 8230 and references cited therein.
[7] a) T. L. Chasse, C. B. Gorman, *Langmuir* **2004**, *20*, 8792; b) T. L. Chasse, R. Sachdeva, Q. Li, Z. Li, R. J. Petrie, C. B. Gorman, *J. Am. Chem. Soc.* **2003**, *125*, 8250.
[8] a) R. Shakya, S. S. Hindo, L. Wu, S. Ni, M. M. Allard, M. J. Heeg, S. R. P. da Rocha, G. T. Yee, H. P. Hratchian, C. N. Verani, *Chem. Eur. J.* **2007**, *13*, 9948; b) R. Shakya, P. H. Keyes, M. J. Heeg, A. Moussawel, P. A. Heiney, C. N. Verani, *Inorg. Chem.* **2006**, *45*, 7587.
[9] a) L. M. C. Beltran, J. R. Long, *Acc. Chem. Res.* **2005**, *38*, 325; b) A. J. Tasiopoulos, A. Vinslava, W. Werndorfer, K. A. Abboud, G. Christou, *Angew. Chem. Int. Ed.* **2004**, *43*, 2117; c) M. Eddaoudi, D. B. Moler, H. Li, B. Chen, T. M. Reineke, M. O'Keeffe, O. M. Yaghi, *Acc. Chem. Res.* **2001**, *34*, 319.
[10] a) D. R. Talham, *Chem. Rev.* **2004**, *104*, 5479; b) J. T. Culp, J.-H. Park, D. Stratakis, M. W. Meisel, D. R. Talham, *J. Am. Chem. Soc.* **2002**, *124*, 10083.
[11] a) Y. Bodenthin, U. Pietsch, H. Moehwald, D. G. Kurth, *J. Am. Chem. Soc.* **2005**, *127*, 3110; b) D. G. Kurth, P. Lehmann, M. Schutte, *Proc. Natl. Acad. Sci. USA* **2000**, *97*, 5704.
[12] a) M. Eddaoudi, D. B. Moler, H. Li, B. Chen, T. M. Reineke, M. O'Keeffe, O. M. Yaghi, *Acc. Chem. Res.* **2001**, *34*, 319; b) S. Kitagawa, R. Kitaura, S.-I. Noro, *Angew. Chem. Int. Ed.* **2004**, *43*, 2334.
[13] N. H. Pilkington, R. Robson, *Aust. J. Chem.* **1970**, *23*, 2225.
[14] a) G. Grasa, F. Tuna, R. Gheorghe, D. B. Leznoff, S. J. Rettig, M. Andruh, *New J. Chem.* **2000**, *24*, 615; b) C. N. Verani, T. Weyhermüller, E. Rentschler, E. Bill, P. Chaudhuri, *Chem. Commun.* **1998**, 2475; c) E. V. Rybak-Akimova, D. H. Busch, P. K. Kahol, N. Pinto, N. Alcock, H. J. Clase, *Inorg. Chem.* **1997**, *36*, 510; d) R. C. Long, D. N. Hendrickson, *J. Am. Chem. Soc.* **1983**, *105*, 1513; e) R. R. Gagne, C. A. Koval, T. J. Smith, *J. Am. Chem. Soc.* **1977**, *99*, 8367.
[15] J. Galvan-Miyoshi, S. Ramos, J. Ruiz-Garcia, R. Castillo, *J. Chem. Phys.* **2001**, *115*, 8178.
[16] S. S. Hindo, R. Shakya, N. S. Rannulu, M. M. Allard, M. J. Heeg, M. T. Rodgers, S. R. P. da Rocha, C. N. Verani, *Inorg. Chem.* **2008**, *47*, 3119.
[17] M. A. Kalinina, V. V. Arslanov, L. A. Tsar'kova, V. D. Dolzhikova, A. A. Rakhnyanskaya, *Colloid J.* **2001**, *63*, 312.
[18] M. C. Petty, *Langmuir-Blodgett Films*, Cambridge Univ. Press, Cambridge, U. K., **1996**, p. 12–38.
[19] A. M. Gonçalves da Silva, J. C. Guerreiro, N. G. Rodrigues, T. O. Rodrigues, *Langmuir* **1996**, *12*, 4442.
[20] M. Sickert, F. Rondelez, H. A. Stone, *Europhys. Lett.* **2007**, *79*, 66005.
[21] G. Baskar, A. B. Mandal, *Langmuir* **2000**, *16*, 3957.
[22] Y. S. Kang, D. K. Lee, Y. S. Kim, *Synth. Met.* **2001**, *117*, 165.
[23] F. Gaboriaud, R. Volinsky, A. Berman, R. Jelinek, *J. Colloid Interface Sci.* **2005**, *287*, 191.
[24] a) G. L. Eichhorn, N. D. Marchand, *J. Am. Chem. Soc.* **1956**, *78*, 2688; b) G. L. Eichhorn, J. C. Bailar Jr., *J. Am. Chem. Soc.* **1953**, *75*, 2905.
[25] P. Lehmann, D. G. Kurth, G. Brezesinski, C. Symietz, *Chem. Eur. J.* **2001**, *7*, 1646.
[26] H. D. Jayathilake, J. A. Driscoll, A. N. Bordenyuk, L. Wu, S. R. P. da Rocha, C. N. Verani, A. V. Benderskii, *Langmuir* **2009**, *25*, 6880.
[27] M. Pascu, M. Andruh, A. Mueller, M. Schmidtmann, *Polyhedron* **2004**, *23*, 673.
[28] *APEX II*, collection and processing programs are distributed by the manufacturer, Bruker AXS Inc., Madison WI, USA.
[29] G. Sheldrick, *SHELX-97*, University of Göttingen, Germany, **1997**.
[30] C. N. Verani, E. Rentschler, T. Weyhermuller, E. Bill, P. Chaudhuri, *J. Chem. Soc., Dalton Trans.* **2000**, 251.
[31] V. Percec, C.-H. Ahn, T. K. Bera, G. Ungar, D. J. P. Yeardley, *Chem. Eur. J.* **1999**, *5*, 1070.
[32] R. R. Gagne, C. A. Koval, T. J. Smith, M. C. Cimolino, *J. Am. Chem. Soc.* **1979**, *101*, 4571.

Received: July 6, 2009
Published Online: September 23, 2009

  